Astron. Astrophys. 364, L31–L35 (2000)

ASTRONOMY AND ASTROPHYSICS

LETTER

Letter to the Editor

Revealing deuterium Balmer lines in H II regions with VLT-UVES*

G. Hébrard[1], **D. Péquignot**[2], **J.R. Walsh**[3], **A. Vidal-Madjar**[1], **and R. Ferlet**[1]

[1] Institut d'Astrophysique de Paris, CNRS, 98 bis Boulevard Arago, 75014 Paris, France (hebrard@iap.fr, vidalmadjar, ferlet)
[2] Laboratoire d'Astrophysique Extragalactique et de Cosmologie associé au CNRS (UMR 8631) et à l'Université Paris 7, DAEC, Observatoire de Paris-Meudon, 92195 Meudon Cédex, France (daniel.pequignot@obspm.fr)
[3] Space Telescope European Co-ordinating Facility, European Southern Observatory, Karl-Schwarzschild-Strasse 2, 85748 Garching bei München, Germany (jwalsh@eso.org)

Received 15 August 2000 / Accepted 25 August 2000

Abstract. The search for deuterium Balmer lines with VLT-UVES is reported in H II regions of the Galaxy and the Magellanic Clouds. The D I lines appear as faint, narrow emission features in the blue wings of the H I Balmer lines and can be distinguished from high-velocity H I emission. The previous identification to deuterium is re-inforced beyond doubt.

The detection of Dα and Dβ in Orion (Hébrard et al. 2000) is confirmed and deuterium lines are now detected up to at least Dη. The UVES observations provide the first detection of Balmer D I lines in four new H II regions (M 8, M 16, M 20, and DEM S 103 in SMC), demonstrating that these lines are of common occurence.

Key words: line: identification – ISM: atoms, ions – ISM: H II regions – ISM: individual objects: M42, M8, M16, M20, M17, DEM S 103

1. Introduction

Deuterium is an element of primordial origin. Measuring its abundance in different astrophysical sites brings valuable constraints on the Big-Bang nucleosynthesis and the Galactic evolution (e.g. Lemoine et al. 1999).

The detection and identification of the deuterium Balmer lines Dα and Dβ in emission in the Orion Nebula was first reported by Hébrard et al. (2000, hereafter Paper I). The narrowness of these lines, their strength with respect to the hydrogen lines and finally their relative fluxes were incompatible with recombination excitation, but could be understood in terms of fluorescence excitation by stellar UV continuum in the Photon Dominated Region (PDR), located behind the ionized region.

Here, observations of the whole Balmer series with the new spectrograph UVES, installed at the Nasmyth focus of VLT-UT2, are presented for Orion and other H II regions. Observations are described in Sect. 2. Results for each H II region are presented in Sect. 3. New evidence in support to the identification of deuterium is discussed in Sect. 4. A more complete analysis will follow in forthcoming papers.

2. Observations

Observations were secured during the night 2000 July 25th-26th, using the UV-Visual Echelle Spectrograph (UVES) located at the Nasmyth focus of Kueyen, the second VLT Unit Telescope (D'Odorico & Kaper 2000). Spectra from both the red and blue arms were registered simultaneously on two detectors, using the standard setting DIC1 (390+564). The approximate spectral ranges were 3290 Å - 4530 Å (blue arm), and 4610 Å - 5620 Å and 5660 Å - 6660 Å (red arm), encompassing the whole Balmer series.

The slits were 8″ and 11″ long for the blue and red arms respectively. The slit width was 1″ on the sky. According to the staff of the VLT, the spectral resolution was $R = \lambda/\Delta\lambda \simeq 40\,000$ (Full Width at Half Maximum, FWHM), equivalent to $\sim\ 7\,\mathrm{km\,s^{-1}}$. The present conclusions do not depend on the exact value of R, which will be determined after reducing the calibration exposures. A total exposure time of one hour was devoted to each H II region (except for Orion, Sect. 3.1), the observations being divided in short sub-exposures to prevent detector saturation at the H I Balmer lines.

Data reduction (bias subtraction, flat-fielding, wavelength calibration) was performed with the UVES pipeline, using the available calibration database. 1D spectra were box-extracted from the central third of the slits. The standard sky-subtraction algorithm, inappropriate for extended objects, was omitted. This extraction was judged robust enough for this preliminary study. Subsequent data reduction will be performed over the whole slit length, using the calibration exposures obtained during the observing run.

Cosmics and bad pixels were cleaned where necessary. Sub-exposures were averaged (no shift was observed from one sub-exposure to the next) and the lines were shifted to the same

Send offprint requests to: Guillaume Hébrard

* Based on observations collected at the European Southern Observatory, Paranal, Chile [ESO VLT-UT2 N^o 65.I-0498(A)].

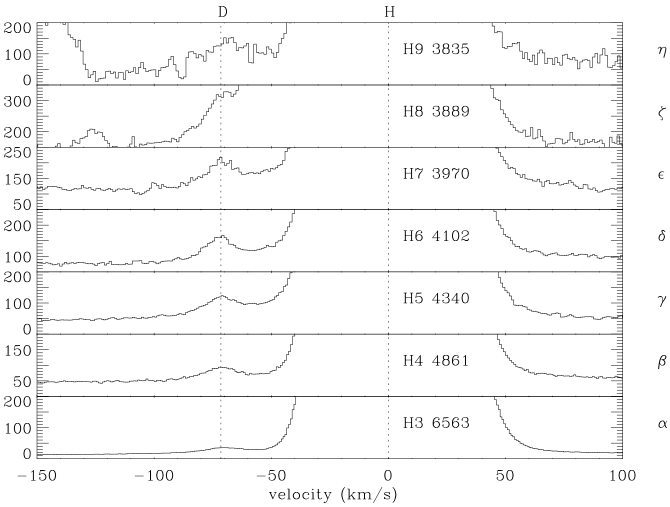

Fig. 1. Wings of Hα to Hη (noted H3 to H9) in the Orion Nebula. All H I lines are centred at $0\,\mathrm{km\,s^{-1}}$ velocity (right dotted line) and are normalized to identical peak intensities (2.1×10^4 on y-scale). The dotted line to the left corresponds to the wavelengths adopted for the D I lines (Table 2). Hζ is blended with He I.

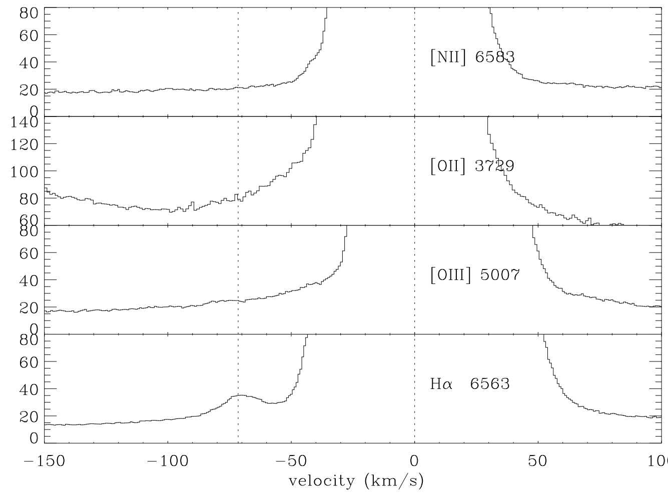

Fig. 2. Same as Fig. 1 for wings of [N II], [O II], [O III] and Hα in Orion (peak intensities $2.1{\times}10^4$). Compare to Fig. 7.

Table 1. Preliminary line flux ratios in M 42

line	D I/H I	line	D I/H I	line	D I/H I
α	2×10^{-4}	γ	7×10^{-4}	ϵ	10×10^{-4}
β	6×10^{-4}	δ	9×10^{-4}		

radial velocity. For a given object, the peak fluxes of the different lines were assigned the same value in order to display the relative variations of the weak lines (figures of Sect. 3). Shifts and normalizations were all based on Gaussian fits to the emission lines.

3. Results

Line detections reported here in the blue wings of the H I lines are at least at the 5-σ confidence level. Most of them are confirmed by the detection of lines at the same velocity for several principal quantum numbers n.

3.1. Orion Nebula (M 42)

The area observed in Orion was the same as the one observed previously (Paper I). The slit, oriented North-South, was located 2.5′ South of θ^1 Ori C (HD 37022) at coordinates α =05:35:16.7, $\delta = -$05:25:29 (J2000). The exposure time was 30 min in the red arm and 50 min in the blue arm.

Plots of the H I Balmer line wings are shown in Fig. 1. Deuterium lines are detected from Dα to Dη. They are redshifted $\sim 10\,\mathrm{km\,s^{-1}}$ with respect to H I (the isotopic shift between D I and H I at rest is $-81.6\,\mathrm{km\,s^{-1}}$), in good agreement with the previous measurements (Paper I). D I lines seem to be detected up to D16, but elaborate treatment is required due to low signal-to-noise ratio.

FWHM are from Gaussian fits, after quadratic subtraction of the instrumental point-spread function. The FWHM of the D I lines is $\sim 11\,\mathrm{km\,s^{-1}}$, much less than that of the H I recombination lines ($\sim 30\,\mathrm{km\,s^{-1}}$). Widths similar to these were found for the lines detected in M 8, M 16, M 20 and DEM S 103 (see below). From Fig. 1, it is apparent that D I increases relative to H I for increasing n, at least up to Dϵ. Approximate relative fluxes are given in Table 1. Despite lower signal-to-noise ratio, a similar trend exists in the data for M 8 and M 16.

In Fig. 2, are shown on the same scale the wings of [N II] λ6583 Å, [O II] λ3729 Å, [O III] λ5007 Å and Hα. No counterparts to D I can be seen for lines other than Hα, thus excluding any interpretation in terms of emission from high-velocity ionized gas (see Sect. 3.6). Similarly, counterparts are lacking in M 8, M 16, M 20 and DEM S 103.

3.2. Lagoon Nebula (M 8)

In M 8, the slit was oriented North-South and located 17″ East and 18″ North of Herschel 36 (HD 164740), at α =18:03:40.8, $\delta = -$24:22:25. This position corresponds to position L11 in Bohuski (1973). Deuterium is detected from Dα to Dζ (Fig. 3). Again the flux ratios range from $F(\mathrm{D}\alpha)/F(\mathrm{H}\alpha) \simeq 2 \times 10^{-4}$ to $F(\mathrm{D}\zeta)/F(\mathrm{H}\zeta) \simeq 1 \times 10^{-3}$.

M 8 was observed at a second slit position: 43″ South from Herschel 36 [position L7 in Bohuski (1973), not shown here]. The coordinates were α =18:03:40.3, $\delta = -$24:23:27 and the slit was oriented East-West. Only Dα was detected, with a weaker flux: $F(\mathrm{D}\alpha)/F(\mathrm{H}\alpha) \simeq 3 \times 10^{-5}$.

3.3. Eagle Nebula (M 16)

In M 16, the slit was oriented North-South and located at α =18:18:51.7, $\delta = -$13:49:07. It corresponds to one of the brightest regions of the PDR in this nebula (Levenson et al. 2000). Deuterium is detected from Dα to Dγ (Fig. 4).

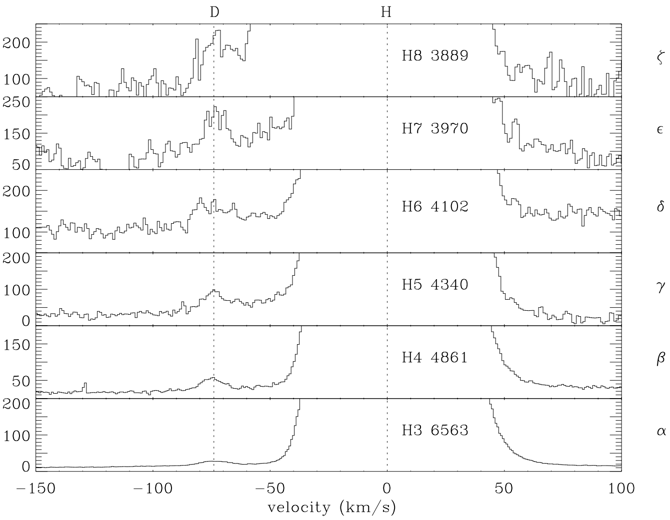

Fig. 3. Same as Fig. 1 for wings of Hα to Hζ in M 8, but with peak intensities $2.0{\times}10^4$.

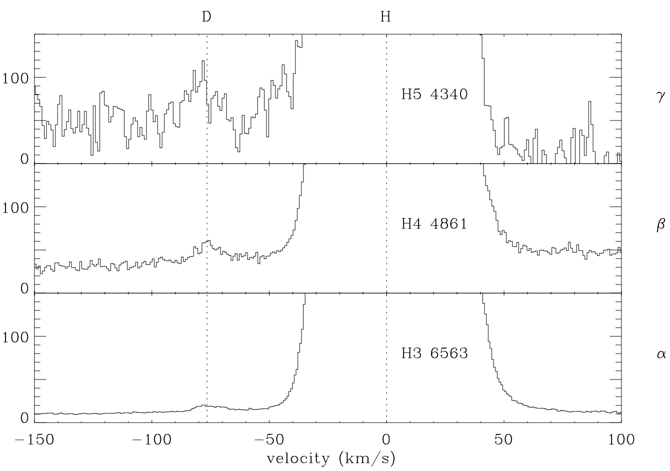

Fig. 4. Same as Fig. 1 for wings of Hα to Hγ in M 16, but with peak intensities 1.1×10^4.

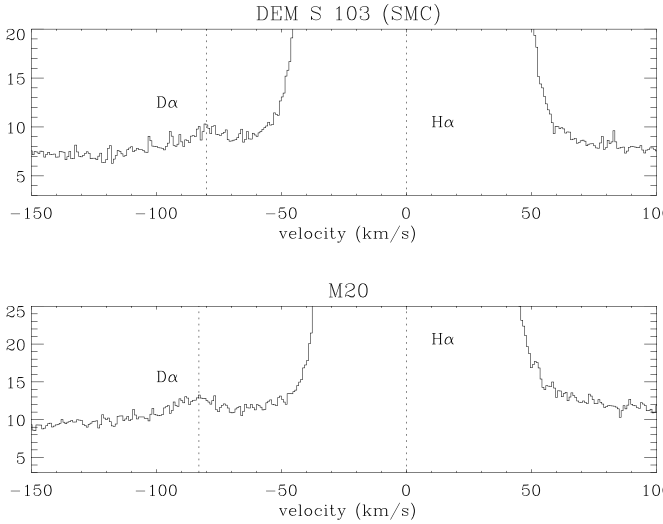

Fig. 5. Same as Fig. 1 for wings of Hα in M 20 (bottom, peak intensity 4000) and DEM S 103 in SMC (up, peak intensity 3500).

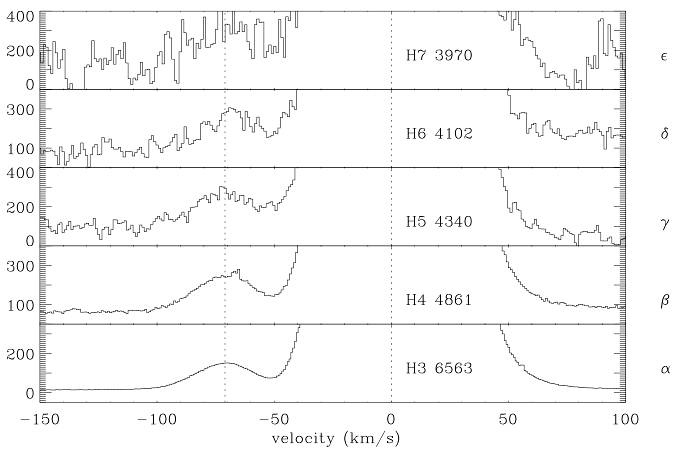

Fig. 6. Same as Fig. 1 for wings of Hα to Hϵ in M 17 (peak intensities 2.1×10^4). Here the blue-shifted features are not identified with D I but with H I emission from a high-velocity ionized structure.

The flux ratios range from $F(\mathrm{D}\alpha)/F(\mathrm{H}\alpha) \simeq 2 \times 10^{-4}$ to $F(\mathrm{D}\gamma)/F(\mathrm{H}\gamma) \simeq 1 \times 10^{-3}$.

3.4. Trifid Nebula (M 20)

In M 20, the slit was oriented North-South and located 51″ East and 23″ South from HD 164492, at α =18:02:27.3, $\delta = -$23:02:14. This position corresponds to position T12 in Bohuski (1973). Only Dα was detected (Fig. 5).

3.5. DEM S 103 in the Small Magellanic Cloud

The last deuterium Balmer line detection was performed outside the Galaxy, in the brightest H II region of the SMC, namely DEM S 103 [Henize 66, Caplan et al. (1996)]. The coordinates of the slit, oriented North-South, were α =00:58:51.6, $\delta =$ $-$72:10:09. Again, only Dα was detected (Fig. 5).

3.6. Omega Nebula (M 17): high-velocity structure emission

In M 17, the slit was oriented North-South and located at α =18:20:48.0, $\delta = -$16:10:31. Here the emission features detected in the blue wings of the H I lines, from Hα to Hϵ (Fig. 6), differ from those shown in previous targets:

- they are broad (FWHM $\simeq$ 20 $\mathrm{km\,s^{-1}}$, instead of $\sim$10 $\mathrm{km\,s^{-1}}$, whilst the main H I component has the usual FWHM $\simeq$ 30 $\mathrm{km\,s^{-1}}$);
- they are proportional to the H I lines (intensity $\sim 3 \times 10^{-3}$ relative to nearby H I for every n);
- [N II], [O II] and [O III] present clear counterparts at the same velocity (Fig. 7).

It is concluded that, in this case, the features should be mainly due to H I emission from ionized material with velocity $\sim -70\,\mathrm{km\,s^{-1}}$ relative to the main body of the nebula. The width of these features is compatible with recombination excita-

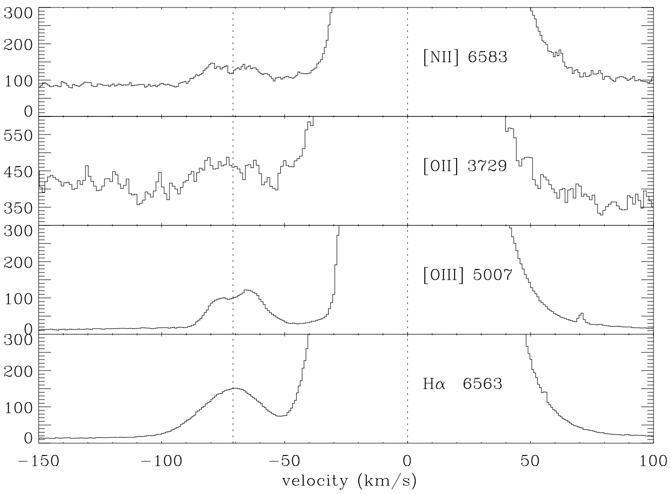

Fig. 7. Same as Fig. 1 for wings of [N II], [O II], [O III] and Hα in M 17 (peak intensities 2.1×10^4). Here, the blue-shifted features have counterparts in ions. Compare to Fig. 2.

Table 2. Kinematic properties of the D I lines[a]

Object	Shift[b]	Width[c]	Object	Shift[b]	Width[c]
M 42	10	11	M 20	-1:	13:
M 8	8	9	S 103	2:	10:
M 16	5	9	M 17	-	-

[a] Colons indicate low-accuracy values (from Hα and Dα only).
[b] Average shift of D I with respect to H I ($\mathrm{km\,s^{-1}}$).
[c] Average FWHM of the D I lines ($\mathrm{km\,s^{-1}}$).

tion in a hot H^+ gas. In fact, Meaburn & Walsh (1981) detected velocity components shifted by $\sim -70\,\mathrm{km\,s^{-1}}$ from the main Hα component, $\sim 2'$ South of the UVES position. Clayton et al. (1985) showed that the high-velocity material was probably associated with a breakout (collimated outflow) of a radially expanding shell. A Dα line with the same relative flux as in Orion would be one order of magnitude weaker than the feature near Hα, making detection difficult without an elaborate treatment.

4. Confirming the identification of deuterium

In addition to the objects presented in Sect. 3, two more H II regions were observed: 30 Doradus (in the LMC) and Sh2-100. In the former, the velocity field appears complex and more work is needed. In the latter, no obvious D I lines are seen, suggesting that no PDR is present along the line of sight. So far, D I lines have therefore been detected in at least five out of the eight H II regions observed. Kinematic properties appear in Table 2.

The new observations bring confirmatory evidence in favour of the identification of the deuterium Balmer lines. They complement and add to the results presented in Paper I. The lines are seen with similar characteristics in the five H II regions, using different telescopes (CFHT and VLT) and different spectrographs (GECKO and UVES). Instrumental artifacts (such as grating ghosts or in-order scattered light) can be definitely ruled out.

Since the lines are seen for many members of the Balmer series, they can only be D I or blue-shifted H I emission. H I emission may arise from H^+ gas (recombination) or H^0 gas (fluorescence). High-velocity ionized structures will produce H I recombination lines with properties like those already listed in the case of M 17 (width, flux, counterparts), not observed in the other H II regions described in Sect. 3. A high-velocity neutral structure cannot be formally excluded for any one isolated object, but the probability that such a structure could exist and yet be detectable only in H I is low. No evidence for the existence of such a structure could be found in the case of Orion (Paper I). Considering the present data, it would be extraordinary if such a neutral component could be present in such a systematic manner in five different H II regions, always at about the same velocity.

Understandably, the D I lines are narrow since they arise from a cold material with small thermal velocity. Nonetheless, considering the prevalence of large velocity fields in H II regions, it was not a priori obvious that these lines would appear so systematically narrow (Table 2). The explanation partly lies in the fact that the entrance aperture of UVES is relatively small and that observable H II regions tend to be incomplete on one side, with the associated molecular cloud and PDR located behind the expanding H^+ region. This is consistent with the tendency shown by the D I lines to be redshifted with respect to the H I lines (Table 2). Thus, in practice, a small line width (at the expected wavelength!) turns out to be an important criterion to identify D I. On the other hand, H II regions may exist with PDR's encompassing a large velocity range. A fundamental criterion for D I identification remains the lack of counterparts in lines from ionized species. Large variations of the line intensity ratio D I/H I with n constitute another useful criterion (Table 1), since fluorescence will generally not result in the same decrement as the one corresponding to recombination.

As a result of the present high spectral resolution and high signal-to-noise observations, the identification of deuterium Balmer lines is now very safe.

5. Conclusion

Detection of deuterium Balmer emission in five H II regions is reported. These are first detections in four targets, including an extragalactic one. Detection was made feasible thanks to the large collecting area of the 8.2m VLT mirror and the high efficiency of UVES. Fluorescence is confirmed as the probable excitation mechanism of D I, recombination being excluded. Spectroscopic criteria leading to virtually certain identification of D I in any given H II region are now clearly established.

Possible ways to determine D/H from D I Balmer lines were discussed in Paper I. One method requires a knowledge of the n for which the line ratio D I/H I starts decreasing. The detection of D I up to D9, and possibly D16, in Orion suggests this as a promising way of investigation. Comparison of D I to O I fluorescence lines, present in the UVES spectra and also produced in the PDR, may be another way to explore.

Acknowledgements. We thank the staff of the VLT for excellent assistance.

References

Bohuski, T. J., 1973, ApJ 183, 851
Caplan, J., Ye, T., Deharveng, L., Turtle, A. J., & Kennicutt, R. C., 1996, A&A 307, 403
Clayton, C. A., Ivchenko, V. N., Meaburn, J., & Walsh, J. R., 1985, MNRAS 216, 761
D'Odorico, S., & Kaper, L., 2000, *UVES User Manual*, V 1.0
Hébrard, G., Péquignot, D., Vidal-Madjar, A., Walsh, J. R., & Ferlet, R., 2000, A&A 354, L79 (Paper I)
Lemoine, M., et al., 1999, *New Astronomy* 4, 231
Levenson, N. A., et al., 2000, ApJ 533, L53
Meaburn, J., & Walsh, J. R., 1981, A&SS 74, 169